

## Resummed Differential Cross Sections for Top-Quark Pairs at the LHC

Benjamin D. Pecjak,<sup>2</sup> Darren J. Scott,<sup>2</sup> Xing Wang,<sup>1</sup> and Li Lin Yang<sup>1,3,4</sup>

<sup>1</sup>*School of Physics and State Key Laboratory of Nuclear Physics and Technology, Peking University, Beijing 100871, China*

<sup>2</sup>*Institute for Particle Physics Phenomenology, University of Durham, DH1 3LE Durham, United Kingdom*

<sup>3</sup>*Collaborative Innovation Center of Quantum Matter, Beijing, China*

<sup>4</sup>*Center for High Energy Physics, Peking University, Beijing 100871, China*

(Received 9 February 2016; revised manuscript received 5 April 2016; published 19 May 2016)

We present state of the art resummation predictions for differential cross sections in top-quark pair production at the LHC. They are derived from a formalism which allows the simultaneous resummation of both soft and small-mass logarithms, which endanger the convergence of fixed-order perturbative series in the boosted regime, where the partonic center-of-mass energy is much larger than the mass to the top quark. We combine such a double resummation at next-to-next-to-leading logarithmic' (NNLL') accuracy with standard soft-gluon resummation at next-to-next-to-leading logarithmic accuracy and with next-to-leading-order calculations, so that our results are applicable throughout the whole phase space. We find that the resummation effects on the differential distributions are significant, bringing theoretical predictions into better agreement with experimental data compared to fixed-order calculations. Moreover, such effects are not well described by the next-to-next-to-leading-order approximation of the resummation formula, especially in the high-energy tails of the distributions, highlighting the importance of all-orders resummation in dedicated studies of boosted top production.

DOI: 10.1103/PhysRevLett.116.202001

The 8 TeV run of the LHC delivered about  $20 \text{ fb}^{-1}$  of integrated luminosity to both the ATLAS and CMS experiments. Among the many important results coming from these data, the properties of the top quark have been measured with unprecedented precision. At the same time, theoretical calculations of top-quark-related observables have seen significant advancements in the past few years. In particular, very recently, the next-to-next-to-leading-order (NNLO) QCD corrections to differential cross sections in top-quark pair ( $t\bar{t}$ ) production have been calculated [1]. In Ref. [2], the CMS Collaboration performed a comprehensive comparison between their measurements [3] of the differential cross sections and various theoretical predictions, including those from the NNLO calculation and those from Monte Carlo event generators with next-to-leading-order (NLO) accuracy matched to parton showers. The overall agreement between the theory and data is truly remarkable, which adds to the success of the standard model (SM) as an effective description of nature.

However, a persistent issue in the 8 TeV results is that the transverse momentum ( $p_T$ ) distribution of the top quark or antiquark is softer in the data than in theoretical predictions; i.e., the experimentally measured differential cross section at high  $p_T$  is lower than predictions from event generators or from NLO fixed-order calculations [3,4]. While the NNLO corrections bring the fixed-order predictions into better agreement with the CMS data, as noted in Refs. [1,2], there is still some discrepancy in the high- $p_T$  bins where  $p_T > 200 \text{ GeV}$ . Given the importance of the  $t\bar{t}$  production process as a standard candle for validating the SM and as an

essential background for new physics searches, it would be disconcerting if this feature were to persist at higher  $p_T$  values and with more data. It is therefore important to assess the effects of QCD corrections even beyond NNLO, in order to see whether the gap between the theory and data at high  $p_T$  can be bridged.

For boosted top-quark pairs with high  $p_T$ , there are two classes of potentially large contributions. The first is the Sudakov-type double logarithms arising from soft-gluon emissions. The second comes from gluons emitted nearly parallel to the top quarks, resulting in large logarithms of the form  $\ln^n(m_t/m_T)$ , where  $m_t$  is the top-quark mass and  $m_T \equiv \sqrt{m_t^2 + p_T^2}$  is the transverse mass of the top quark or antiquark. In Ref. [5], some of the authors of the current work developed a formalism for the simultaneous resummation of both type of logarithms to all orders in the strong coupling constant  $\alpha_s$ . In this Letter, we report the first phenomenological applications of that formalism, giving predictions for the  $t/\bar{t}$   $p_T$  and the  $t\bar{t}$  invariant mass distributions at the 8 TeV LHC and comparing with experimental measurements as well as the NNLO calculations when possible. With an eye to the future, we also present predictions for the 13 TeV LHC, where NNLO results are not yet available.

Our main finding is that the higher-order effects contained in our resummation formalism significantly alter the high-energy tails of the  $p_T$  and  $t\bar{t}$  invariant mass distributions, softening that of the  $p_T$  distribution but enhancing that of the  $t\bar{t}$  invariant mass distribution. These effects bring our results into better agreement with the experimental data

compared to pure NLO fixed-order calculations. Interestingly, for the case of the  $p_T$  distribution, this softening of the spectrum is slightly stronger than the similar effect displayed in recent NNLO results and leads to a better modeling of the  $p_T > 200$  GeV portion of the CMS data [3]. We comment further on this fact in the conclusions.

*Formalism.*—Our predictions are based on the factorization and resummation formula derived in Ref. [5]. The technical details will be given in a forthcoming paper, although the main elements have already been sketched out in Ref. [6]. In the kinematic situation where the top quarks are highly boosted and the events are dominated by soft-gluon emissions, the resummed partonic differential cross section in Mellin space can be written as

$$\begin{aligned} & \tilde{c}_{ij}(N, M_{\bar{t}t}, m_t, \mu_f) \\ &= \text{Tr} \left[ \tilde{U}_{ij}(\mu_f, \mu_h, \mu_s) \mathbf{H}_{ij}(M_{\bar{t}t}, \mu_h) \right. \\ & \quad \times \tilde{U}_{ij}^\dagger(\mu_f, \mu_h, \mu_s) \tilde{s}_{ij} \left( \ln \frac{M_{\bar{t}t}^2}{\bar{N}^2 \mu_s^2}, \mu_s \right) \left. \right] \\ & \quad \times \tilde{U}_D^2(\mu_f, \mu_{dh}, \mu_{ds}) C_D^2(m_t, \mu_{dh}) \tilde{s}_D^2 \left( \ln \frac{m_t}{\bar{N} \mu_{ds}}, \mu_{ds} \right), \quad (1) \end{aligned}$$

where, for simplicity, we have suppressed some variables in the functional arguments which are unnecessary for the explanations below. In the above formula,  $M_{\bar{t}t}$  is the invariant mass of the  $t\bar{t}$  pair (which can be related to the  $p_T$  of the top quark or antiquark in the soft limit through a change of variables),  $N$  is the Mellin moment variable dual to  $1 - M_{\bar{t}t}^2/\hat{s}$  with  $\hat{s}$  the partonic center-of-mass energy squared, and  $\bar{N} \equiv N e^{\gamma_E}$  with  $\gamma_E$  the Euler constant. The soft limit corresponds to  $N \rightarrow \infty$  in Mellin space. The four coefficient functions  $\mathbf{H}_{ij}$ ,  $\tilde{s}_{ij}$ ,  $C_D$ , and  $\tilde{s}_D$  encode contributions from four widely separated energy scales  $M_{\bar{t}t}$ ,  $M_{\bar{t}t}/\bar{N}$ ,  $m_t$ , and  $m_t/\bar{N}$ , respectively. The presence of the four scales leads to the two types of large logarithms discussed in the introduction. In correspondence with these four physical scales, there are four unphysical renormalization scales  $\mu_h$ ,  $\mu_s$ ,  $\mu_{dh}$ , and  $\mu_{ds}$ , one for each coefficient function. The philosophy of resummation is to choose the four unphysical scales to be around their corresponding physical scales, so that the four coefficient functions are free of large logarithms and are well behaved in the fixed-order perturbation theory. One can then use renormalization group (RG) equations to evolve these functions to the factorization scale  $\mu_f$  in order to convolute with the parton distribution functions (PDFs) and obtain the hadronic cross sections. The effects of the RG running are encoded in the two evolution factors  $\tilde{U}_{ij}$  (for  $\mathbf{H}_{ij}$  and  $\tilde{s}_{ij}$ ) and  $\tilde{U}_D$  (for  $C_D$  and  $\tilde{s}_D$ ), which resum all the large logarithms to all orders in  $\alpha_s$  in an exponential form.

At the moment, the four coefficient functions are known to NNLO [5,7,8], while the two evolution factors are known to next-to-next-to-leading logarithmic (NNLL) accuracy [5]. Such a level of accuracy is usually referred to as NNLL' in the literature, and we adopt that nomenclature here. While the formula (1) is applicable only in the boosted soft limit, we can extend its domain of validity by combining it with information from NNLL soft-gluon resummation derived in Ref. [9] (recast into Mellin space) as well as the NLO fixed-order result calculated in Ref. [10] and implemented in MCFM [11]. The precise matching formula can be found in Ref. [6]. After such a matching procedure, we denote the final accuracy of our predictions, which are valid throughout phase space, as NLO + NNLL'. (Ideally, we should also match to a purely boosted formula in order to resum small-mass logarithms due to hard-collinear gluon emissions and thus subleading in the soft limit. However, the numerical study in Ref. [5] indicated that such logarithms are not very important for top-quark production at the LHC, so we leave this issue aside in the current study.)

It would be desirable to match with the recent NNLO results in Ref. [1] to achieve NNLO + NNLL' accuracy. However, at the moment, NNLO results are available only for fixed (i.e., kinematics-independent) factorization and renormalization scales  $\mu_f \sim \mu_r \sim m_t$ , whereas for the study of differential distributions over large ranges of phase space we consider it important to follow common practice and use dynamical (i.e., kinematics-dependent) scale choices. Therefore, such an improvement over our result is not currently possible, and we leave it for the future.

*Phenomenology.*—In the following, we present NLO + NNLL' predictions for the  $M_{\bar{t}t}$  and  $p_T$  distributions at the LHC. In all our numerics, we choose  $m_t = 173.2$  GeV and use MSTW2008 NNLO PDFs [12]. For  $p_T$  distributions, the default values for the factorization scale and the four renormalization scales are chosen as  $\mu_f = m_T$ ,  $\mu_h = M_{\bar{t}t}$ ,  $\mu_s = M_{\bar{t}t}/\bar{N}$ ,  $\mu_{dh} = m_t$ , and  $\mu_{ds} = m_t/\bar{N}$ . For  $M_{\bar{t}t}$  distributions, the only difference is  $\mu_f = M_{\bar{t}t}$ . We estimate scale uncertainties by varying the five scales around their default values by factors of 2 and combining the resulting variations of differential cross sections in quadrature; we do not consider uncertainties from PDFs and  $\alpha_s$  in this Letter. The hadronic differential cross sections are first evaluated in Mellin space at a given point in phase space, and we then perform the inverse Mellin transform numerically using the minimal prescription [13]. This procedure relies on an efficient construction of Mellin-transformed parton luminosities, for which we use methods outlined in Refs. [14,15].

The differential cross sections considered below span several orders of magnitude when going from low to high values of  $p_T$  or  $M_{\bar{t}t}$ . In order to better display the relative sizes of various results, we show in the lower panel of each

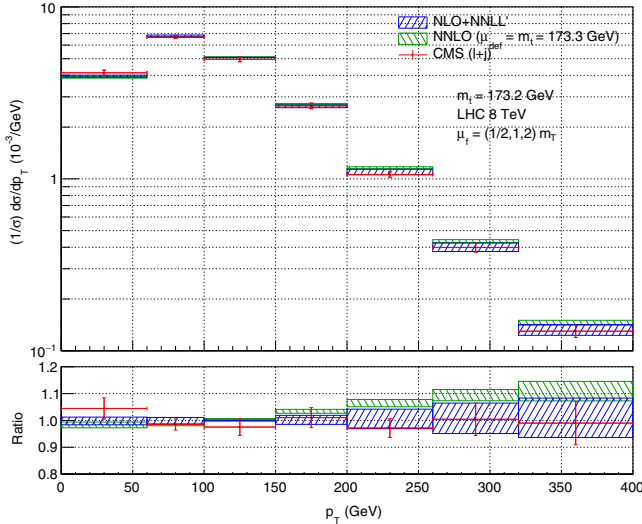


FIG. 1. Resummed prediction (blue band) for the normalized  $p_T$  distribution at the 8 TeV LHC compared with CMS data (red crosses) [3] and the NNLO result (green band) [1]. The lower panel shows results normalized to the default NLO + NNLL' prediction.

plot the differential cross sections normalized to our default prediction, i.e., the ratio defined by

$$\text{ratio} \equiv \frac{d\sigma}{d\sigma^{\text{NLO+NNLL}'(\mu_i = \mu_i^{\text{default}})}}. \quad (2)$$

Figure 1 compares our NLO + NNLL' resummed prediction for the normalized  $p_T$  distribution to the CMS measurement [3] in the lepton + jet channel at the LHC with a center-of-mass energy  $\sqrt{s} = 8$  TeV. Also shown is the NNLO result from Ref. [1], which adopted by default the renormalization and factorization scales  $\mu_r = \mu_f = m_t$  and also used a slightly different top-quark mass,  $m_t = 173.3$  GeV. At low  $p_T$ , it is clear that both the NLO + NNLL' and the NNLO results describe the data fairly well. With the increase of  $p_T$ , it appears that the NNLO prediction systematically overestimates the data, although there is still agreement within errors. On the other hand, with the simultaneous resummation of the soft-gluon logarithms and the mass logarithms and also with the dynamical scale choices, our NLO + NNLL' resummed formula produces a softer spectrum which agrees well with the data.

In Ref. [4], the ATLAS Collaboration carried out a measurement of the  $p_T$  spectrum in the highly boosted region using fat-jet techniques. Although the experimental uncertainty is rather large due to limited statistics, it is interesting to compare it with the theoretical predictions here, since it is expected that the soft and small-mass logarithms become more relevant at higher energies. In Fig. 2, we show such a comparison. The NNLO result for such high  $p_T$  values is not yet available, so we compare

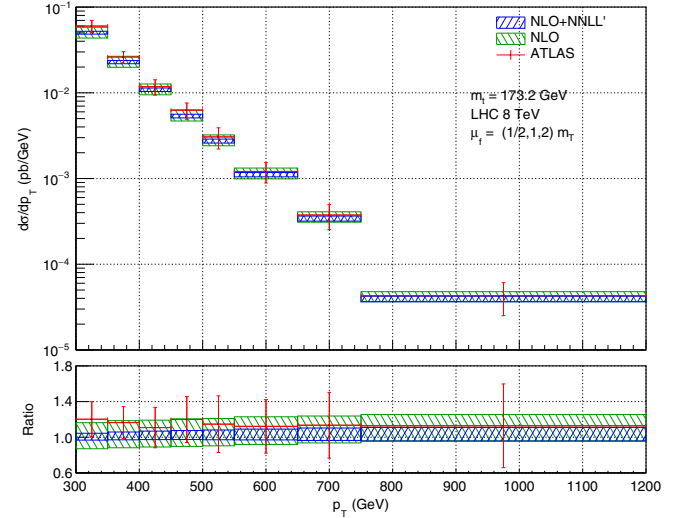


FIG. 2. Resummed prediction (blue band) for the absolute  $p_T$  distribution at the 8 TeV LHC in the boosted region compared with the ATLAS data (red crosses) [4] and the NLO result (green band).

instead with the NLO result computed using MCFM with MSTW2008 NLO PDFs and dynamical renormalization and factorization scales, whose default values are  $\mu_r = \mu_f = m_T$ . Scale uncertainties of the NLO results are estimated through variations of  $\mu_r = \mu_f$  by a factor of 2 around the default value. From the plot, one can see that the NLO result calculated in this way does a good job in estimating the residual uncertainty from higher-order corrections, as the resummed band lies almost inside the NLO one up to  $p_T = 1.2$  TeV. On the other hand, the inclusion of the higher-order logarithms in the NLO + NNLL' result significantly reduces the theoretical uncertainty, which is crucial for future high-precision experiments at the LHC.

Our formalism is flexible and can be applied to other differential distributions as well. To demonstrate this fact, in Fig. 3, we show the NLO + NNLL' resummed prediction for the top-quark pair invariant mass distribution along with a measurement from the ATLAS Collaboration [16] at the 8 TeV LHC. Since the NNLO result in Ref. [1] for this distribution has an incompatible binning, it is currently not possible to include it in the plot, so we show instead the NLO result computed with the same input as in Fig. 2, but this time with the default scale choice  $\mu_r = \mu_f = M_{\bar{t}t}$ . One can see from the plot that the NLO result with this scale choice is consistently lower than the experimental data. The resummation effects significantly enhance the differential cross sections, especially at high  $M_{\bar{t}t}$ . As a result, the NLO + NNLL' prediction agrees with the data quite well. We have found that choosing the default renormalization and factorization scales to be half the invariant mass increases the fixed-order cross section and therefore mimics to some extent the resummation effects. In fact, this

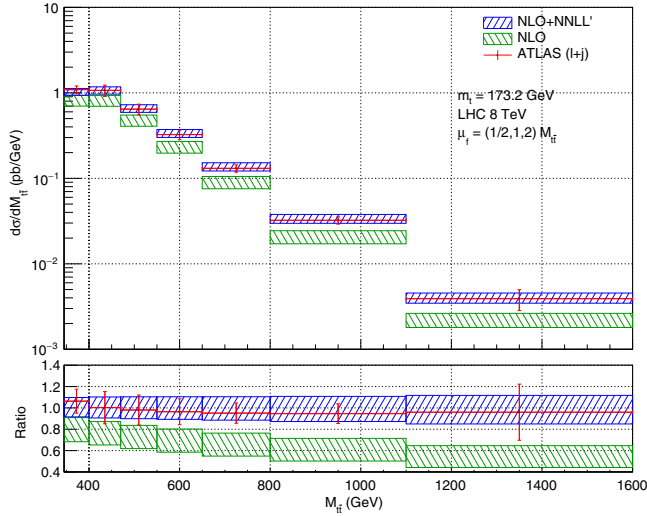


FIG. 3. Resummed prediction (blue band) for the absolute  $M_{t\bar{t}}$  distribution at the 8 TeV LHC compared with ATLAS data (red crosses) [16] and the NLO result (green band).

procedure has been extensively employed in the literature for processes such as Higgs production [17], where higher-order corrections are also large. Consequently, it may be advisable to employ a renormalization and factorization scale of the order of  $M_{t\bar{t}}/2$  in fixed-order calculations (and Monte Carlo event generators), and we shall use this choice when studying the  $M_{t\bar{t}}$  distribution at the 13 TeV LHC below.

The LHC has started the 13 TeV run in 2015. So far, there are only two CMS measurements [18,19] of differential cross sections for  $t\bar{t}$  production, based on just  $42 \text{ pb}^{-1}$  of data. The resulting experimental uncertainties are therefore quite large, and it is not yet possible to probe higher  $p_T$  or  $M_{t\bar{t}}$  values. Nevertheless, in the near future there will be a large amount of high-energy data, which will enable high-precision measurements of  $t\bar{t}$  kinematic distributions, also in the boosted regime. In Fig. 4, we show our predictions for the  $p_T$  and  $M_{t\bar{t}}$  spectrum up to  $p_T = 2 \text{ TeV}$  and  $M_{t\bar{t}} = 4.34 \text{ TeV}$ , contrasted with the NLO results. Note that, for the  $M_{t\bar{t}}$  distribution, we have changed the default  $\mu_f$  to a lower value  $M_{t\bar{t}}/2$  for the reasons explained above. The plots exhibit similar patterns as observed at 8 TeV, namely, that the higher-order resummation effects serve to soften the tail of the  $p_T$  distribution but enhance that of the  $M_{t\bar{t}}$  distribution compared to a pure NLO calculation.

As mentioned before, we would like to match our calculations with the NNLO results when they become available in the future. We end this section by discussing the expected effects of such a matching, by estimating the size of resummation corrections beyond NNLO. We do this in Fig. 5, where the relative sizes of the beyond-NNLO corrections generated through the resummation formula are displayed as a function of  $M_{t\bar{t}}$  or  $p_T$  with the default scale

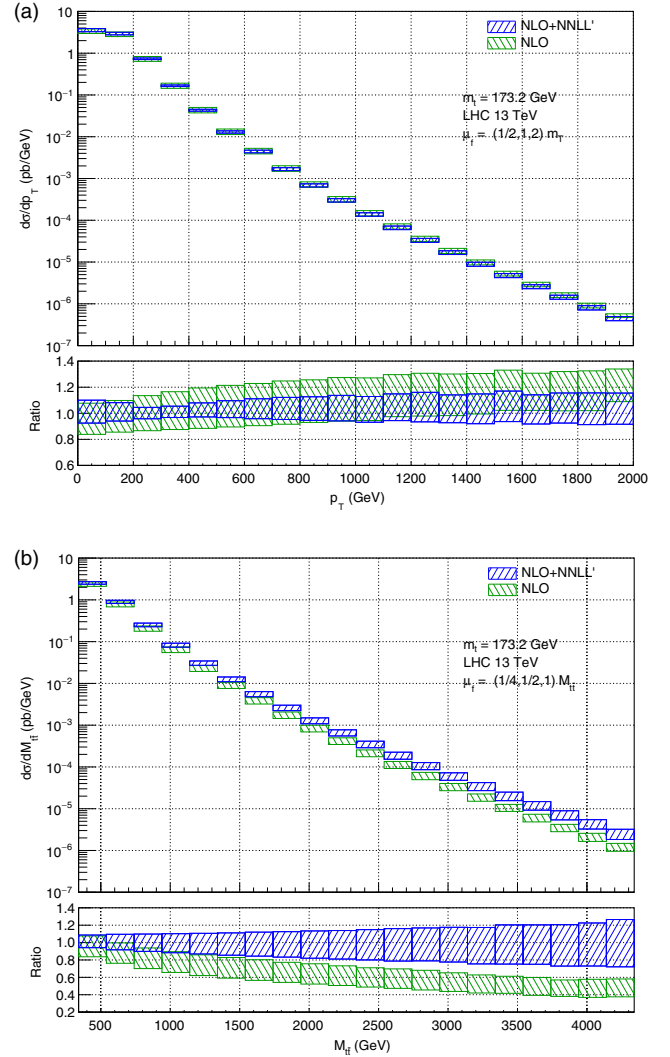


FIG. 4. Resummed predictions (blue bands) for the  $p_T$  and  $M_{t\bar{t}}$  distributions at the 13 TeV LHC compared with the NLO results (green bands).

choices. The exact NNLO results for these scale choices are not yet available, so we show in comparison the relative sizes of the approximate NNLO (aNNLO) corrections obtained by expanding and truncating our NLO + NNLL' formula to that order. More precisely, the blue and black curves in Fig. 5 correspond to

$$\begin{aligned} \text{aNNLO correction} &\equiv \frac{d\sigma^{\text{aNNLO}} - d\sigma^{\text{NLO}}}{d\sigma^{\text{NLO}}}, \\ \text{beyond NNLO} &\equiv \frac{d\sigma^{\text{NLO+NNLL}' } - d\sigma^{\text{aNNLO}}}{d\sigma^{\text{NLO}}}, \end{aligned} \quad (3)$$

where  $d\sigma^{\text{aNNLO}}$  refers to the approximate NNLO result. The figure clearly shows that corrections beyond NNLO are significant in the tails of the distributions, especially in the case of the  $M_{t\bar{t}}$  distribution.



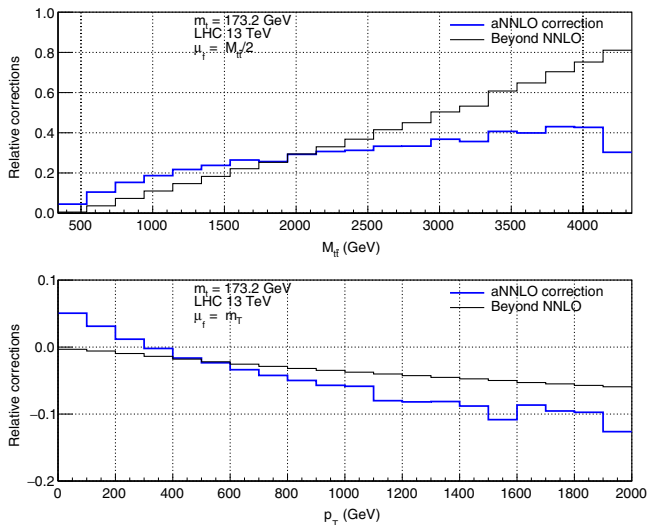


FIG. 5. Relative sizes of the corrections at approximate NNLO (blue) and beyond (black), with respect to NLO. See Eq. (3) and the explanations there for precise definitions.

*Conclusions and outlook.*—In this Letter, we have presented new resummation predictions for differential cross sections in  $t\bar{t}$  production at the LHC. The predictions include the simultaneous resummation to NNLL' accuracy of both soft and small-mass logarithms, which endanger the convergence of the fixed-order perturbative series in the boosted regime where the partonic center-of-mass energy is much larger than the mass of the top quark. This resummation is matched with both standard soft-gluon resummation at NNLL accuracy and fixed-order NLO calculations, so that our results are applicable in the whole phase space. Such predictions for  $t\bar{t}$  differential distributions at the LHC are not only the first to be calculated in Mellin space but also represent the highest resummation accuracy achieved to date, namely, NLO + NNLL'. The results in this Letter build upon previous works [5,9], going beyond them by providing a unified framework and numerical predictions valid for all kinematic configurations of interest. Our results are thus a major step forward in the modeling of distributions, particularly their high-energy tails, which are of great importance for new physics searches.

The agreement of NLO + NNLL' predictions with the data indicates the value of including resummation effects and using dynamical scale settings correlated with  $p_T$  or  $M_{t\bar{t}}$  when studying differential distributions. Interestingly, in the case of normalized  $p_T$  distribution measured by the CMS Collaboration [3], the NLO + NNLL' calculation produces a slightly softer spectrum than recent NNLO predictions (which use a fixed scale setting where  $\mu_f = \mu_r = m_t$  by default), thus achieving a better agreement with the data. However, we emphasize that the optimal use of

resummation is to supplement NNLO calculations, not to replace them. With this in mind, we have studied the size of corrections beyond NNLO encoded in our resummation formula and found that their effects are significant in the high-energy tails of distributions, especially for the  $t\bar{t}$  invariant mass distribution where they enhance the differential cross section. It will therefore be an essential and informative exercise to produce NNLO + NNLL' predictions once NNLO calculations are available with dynamical scale settings.

We thank Alexander Mitov for providing us the results of the NNLO calculations in Ref. [1]. We are grateful to Andrea Ferroglia for collaboration on many related works. X. W. and L. L. Y. are supported in part by the National Natural Science Foundation of China under Grant No. 11575004. D. J. S. is supported by an STFC Postgraduate Studentship.

- 
- [1] M. Czakon, D. Heymes, and A. Mitov, *Phys. Rev. Lett.* **116**, 082003 (2016).
  - [2] CMS Collaboration, Report No. CMS-PAS-TOP-15-011.
  - [3] V. Khachatryan *et al.* CMS Collaboration, *Eur. Phys. J. C* **75**, 542 (2015).
  - [4] G. Aad *et al.* (ATLAS Collaboration), *Phys. Rev. D* **93**, 032009 (2016).
  - [5] A. Ferroglia, B. D. Pecjak, and L. L. Yang, *Phys. Rev. D* **86**, 034010 (2012).
  - [6] A. Ferroglia, B. D. Pecjak, D. J. Scott, and L. L. Yang, *arXiv:1512.02535*.
  - [7] A. Broggio, A. Ferroglia, B. D. Pecjak, and Z. Zhang, *J. High Energy Phys.* **12** (2014) 005.
  - [8] A. Ferroglia, B. D. Pecjak, and L. L. Yang, *J. High Energy Phys.* **10** (2012) 180.
  - [9] V. Ahrens, A. Ferroglia, M. Neubert, B. D. Pecjak, and L. L. Yang, *J. High Energy Phys.* **09** (2010) 097.
  - [10] P. Nason, S. Dawson, and R. K. Ellis, *Nucl. Phys.* **B327**, 49 (1989); M. L. Mangano, P. Nason, and G. Ridolfi, *Nucl. Phys.* **B373**, 295 (1992); S. Frixione, M. L. Mangano, P. Nason, and G. Ridolfi, *Phys. Lett. B* **351**, 555 (1995).
  - [11] J. M. Campbell and R. K. Ellis, *Nucl. Phys. B, Proc. Suppl.* **205–206**, 10 (2010).
  - [12] A. D. Martin, W. J. Stirling, R. S. Thorne, and G. Watt, *Eur. Phys. J. C* **63**, 189 (2009).
  - [13] S. Catani, M. L. Mangano, P. Nason, and L. Trentadue, *Nucl. Phys.* **B478**, 273 (1996).
  - [14] M. Bonvini and S. Marzani, *J. High Energy Phys.* **09** (2014) 007.
  - [15] M. Bonvini, *arXiv:1212.0480*.
  - [16] G. Aad *et al.* (ATLAS Collaboration), *arXiv:1511.04716*.
  - [17] C. Anastasiou, C. Duhr, F. Dulat, F. Herzog, and B. Mistlberger, *Phys. Rev. Lett.* **114**, 212001 (2015).
  - [18] CMS Collaboration, Report No. CMS-PAS-TOP-15-005.
  - [19] CMS Collaboration, Report No. CMS-PAS-TOP-15-010.